

A NUMERICAL ANALYSIS OF THE IN-BORE MOTION OF SMALL CALIBER PROJECTILES

Bernd Dutschke, Martin Hunzinger and Axel Sattler

Fraunhofer Institute for High-Speed-Dynamics, Ernst-Mach-Institut, EMI, Am Christianswuh 2, 79400 Kandern, Germany

Finite Element simulations have become a popular tool to investigate the mechanisms of launch dynamics. However, the common techniques for evaluating the simulation results in terms of target impact accuracy are far from ideal. This paper presents a method for the postprocessing of such simulations. The approach is based on a decomposition of the bullet's transverse motion during launch into a regular rotation caused by the rifling, irregular oscillations (balloting) and muzzle motion. Target impact dispersion is evaluated separately for each of these motion components, which provides a deeper understanding of the dynamic processes determining the weapon's hit performance. In contrast to traditional methods, where the assessment of dispersion requires large numbers of simulations with varying launch conditions, the evaluation of accuracy is based on a single simulation.

INTRODUCTION

In small caliber weapons, the interaction between barrel and projectile during the launch event cannot be captured in a purely experimental manner. Although barrel vibrations can be accessed via strain gauges, laser-vibrometers or image-correlation techniques, measurement of the bullet's transverse motion during firing remains an unsolved problem. On-board accelerometers, which have successfully been used in large caliber weapons [1], are not readily available for small calibers due to the prevalent space limitations. This necessitates the use of numerical simulations to investigate the transverse motion of the projectile during the launch cycle. Three-dimensional, continuum-based Finite Element (FE) modelling of barrel and projectile has become a state of the art technique for both large caliber weapons [2, 3] and small arms [4, 5].

This paper presents a method of analyzing such in-bore simulations in terms of target impact accuracy. It is based on a decomposition of the bullet's transverse motion during launch into a regular rotation caused by the rifling, irregular balloting oscillations and muzzle motion. Target impact dispersion is evaluated separately for each of these motion components, which provides a deeper understanding of the dynamic processes determining the weapon's hit performance. In contrast to the classical approach, where the assessment of dispersion requires large numbers of simulations with varying launch conditions, the method gives an estimation on accuracy from a single simulation.

The first section of the paper gives a brief overview of the Finite Element model utilized to study the launch dynamics of a standard full metal jacket (FMJ) bullet in a 7.62 x 51 mm gun barrel. In the second paragraph, the procedure of decomposing the bullet's transverse motion into three distinct components is presented. Dispersion measures for each of the components are derived in the third section. The paper

concludes with some exemplary results. In particular, the effect of bullet misalignment and the influence of projectile material are addressed.

LAUNCH DYNAMICS FINITE ELEMENT MODEL

The purpose of the model is to study accuracy-affecting mechanisms of launch dynamics in small caliber weapons. The model was set up in Ansys Autodyn and makes use of the software's extensive customization capabilities via user subroutines.

FE Model

Geometry was kept simple and includes projectile, cartridge case and a rifled barrel chambered in 7.62 x 51 mm, as depicted in Figure 1. The barrel is 560 mm in length, with an outer diameter of 20 mm and a 1:12" twist. The cartridge, known as DM111, comprises a standard full metal jacket bullet similar to the M80 ball. Additional components like stock or scope were deliberately omitted in order to isolate the effect of ammunition-specific perturbations. Instead, fixed boundary conditions were assigned to the outer surface of the barrel in the region of the chamber.

For the sake of efficiency, the mesh almost exclusively comprises hexahedron elements, with the exception of some pentahedrons in the region of the forcing cone. The whole model contains about 1.6 M elements.

The barrel consists of steel (42CrMo4), whereas the projectile has a steel jacket (DC04) and a lead antimony core (PbSB3). The cartridge case is made of brass (CuZn30). All materials were modeled elasto-plastic (Johnson-Cook or Steinberg-Guinan) with the parameters taken from literature and Autodyn's material library.

The effect of the burning propellant is incorporated through pressure boundary conditions on the bullet base and the interior surfaces of barrel and cartridge case. Pressure vs. time data were obtained from firing experiments. Note that the pressure may only be applied to the segment of the barrel behind the projectile. The pressure gradient due to acceleration of the propellant gases is also considered. Pressure is therefore a function of time, space and the position of the bullet. Since this type of boundary is not available within Autodyn, a user subroutine (EXSTR3) has been written.

Coulomb friction was applied for the contact between projectile and barrel. The coefficient of friction was obtained from a calibration procedure, where the friction coefficient in the model was varied until the calculated velocity matched the experimental value. The determined value is consistent with the literature. Contact between jacket and core was modelled rigid by means of shared interface nodes.

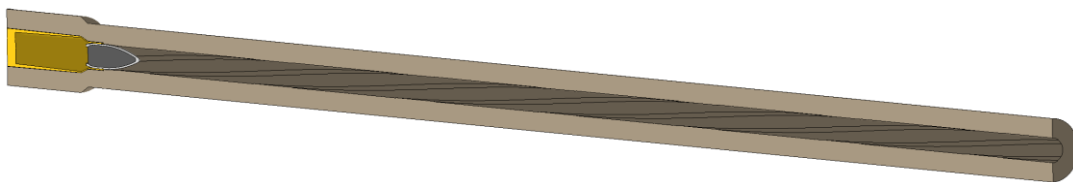


Figure 1. Geometry of the model.

Motion State Output

A major issue with FE launch dynamics simulations is that the code does not provide the information needed for a sophisticated evaluation of dispersion. In order to calculate the impact location, initial flight conditions are required, and those are given by the rigid body motion state of the bullet. Therefore, the subroutine EXEDIT3 was employed to calculate the current rigid body motion of the projectile at each time step, along with the transverse deflection of the barrel centerline.

The rigid body motion of the bullet includes the center of gravity (CG) position and velocity, as well as the direction of the bullet axis and the angular velocity.

The CG position \vec{x}_{CG} is given by the mass-weighted average of all nodal positions \vec{x}_i inside the bullet, while the CG velocity is the respective time derivative

$$\vec{x}_{CG} = \sum \vec{x}_i m_i / m, \quad \vec{v}_{CG} = \dot{\vec{x}}_{CG}. \quad (1)$$

The bullet axis unit vector \vec{e}_1 is calculated as the eigenvector associated with the smallest eigenvalue of the bullet's inertia tensor. The formulas are omitted here, for the sake of brevity, but can be obtained from any textbook on rigid body dynamics.

The projectile's angular velocity $\vec{\omega}$ is usually decomposed into a component $p\vec{e}_1$ along the bullet axis and a transverse component $\vec{\omega}_\perp$

$$\vec{\omega} = p\vec{e}_1 + \vec{\omega}_\perp, \quad p = \vec{\omega} \cdot \vec{e}_1, \quad \vec{\omega}_\perp = \vec{\omega} - p\vec{e}_1. \quad (2)$$

The transverse component $\vec{\omega}_\perp$ can be determined from \vec{e}_1 and its derivative $\dot{\vec{e}}_1$, while p is given by the twist rate L (length per turn) and \vec{v}_{CG} , provided there is no slip between bullet and rifling

$$\vec{\omega}_\perp = \vec{e}_1 \times \dot{\vec{e}}_1, \quad p \cong 2\pi \vec{v}_{CG} / L. \quad (3)$$

In order to track the motion of the barrel centerline, the barrel is sliced into a number of N evenly spaced segments, as depicted in Figure 2. For each segment $j = 1..N$, the mass-weighted average position \vec{x}_j is calculated, which yields a discretized representation of the barrel's deflection curve.

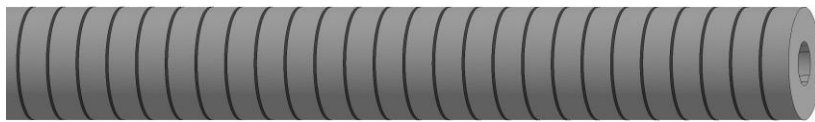


Figure 2. Barrel segments defining the centerline.



Figure 3. Cartridge with tilted projectile.

Perturbations

The Model can be run with different types of perturbations. Examples are projectile imbalance, asymmetric base pressure or different kinds of assembly misalignment. In the following, the analysis procedure is illustrated by means of an exemplary simulation with the projectile initially tilted by 1.0° , as shown in Figure 3.

LAUNCH DYNAMICS ANALYSIS

Projectile Transverse Motion

In order to gain a profound understanding of the dynamic processes that are crucial for accuracy, a thorough analysis of the transverse motion during launch is essential.

The first step is to isolate the projectile motion from the barrel vibrations. To this end, the bullet motion is expressed relative to a moving coordinate system $\vec{e}_{x,y,z}$, which has its origin on and the x -axis aligned with the current barrel centerline (see Figure 4). The origin \vec{x}_0 of the moving coordinate system is given by $\vec{x}_0 = \vec{x}_{BC}(X_{CG})$, where $\vec{x}_{BC}(X)$ is the space curve of the barrel centerline, parametrized by the global coordinate X , and X_{CG} is the X -coordinate of the projectile's CG. The unit vectors $\vec{e}_{x,y,z}$ are

$$\vec{e}_x = \frac{d\vec{x}_{BC}(X_{CG})/dX}{\|d\vec{x}_{BC}(X_{CG})/dX\|}, \quad \vec{e}_y = \vec{e}_z \times \vec{e}_x, \quad \vec{e}_z = \vec{e}_x \times \vec{e}_y. \quad (4)$$

Remember that uppercase indices X, Y, Z refer to the global coordinate system, whereas the moving system is marked with lowercase letters x, y, z . The components of the CG position relative to the moving $\vec{e}_{x,y,z}$ -system are then given by

$$x_{CG} = \vec{e}_x \cdot (\vec{x}_{CG} - \vec{x}_0), \quad y_{CG} = \vec{e}_y \cdot (\vec{x}_{CG} - \vec{x}_0), \quad z_{CG} = \vec{e}_z \cdot (\vec{x}_{CG} - \vec{x}_0), \quad (5)$$

while the direction of the bullet axis is expressed as

$$e_{1,x} = \vec{e}_x \cdot \vec{e}_1, \quad e_{1,y} = \vec{e}_y \cdot \vec{e}_1, \quad e_{1,z} = \vec{e}_z \cdot \vec{e}_1. \quad (6)$$

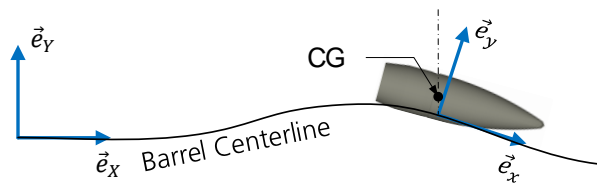


Figure 4. Moving coordinate system to isolate the projectile transverse motion relative to the barrel.

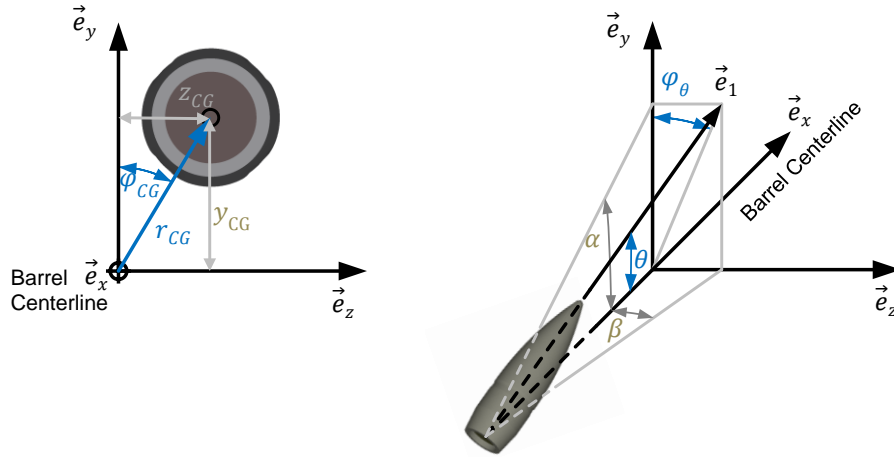


Figure 5. Polar coordinate representation of center of gravity position (left) and bullet tilt (right).

As the angle of bullet tilt is expected to be small, the approximations

$$e_{1,x} \cong 1, \quad e_{1,y} \cong \alpha, \quad e_{1,z} \cong \beta, \quad (7)$$

hold, where α, β denote the bullet's projection angle in the vertical (pitch) and horizontal (yaw) plane (see Figure 5 right).

The corresponding rates (CG velocity and transverse angular velocity) can be obtained via differentiation, as stated by Formulas 1 and 3. The components of the relative CG velocity are therefore given by $(\dot{x}_{CG}, \dot{y}_{CG}, \dot{z}_{CG})$, whereas, with the small angle assumption, the relative transverse angular velocity is $(0, -\dot{\beta}, \dot{\alpha})$.

REGULAR TRANSVERSE MOTION

It is now advantageous to express the relative center of gravity position by means of polar coordinates

$$r_{CG} = \sqrt{y_{CG}^2 + z_{CG}^2}, \quad \varphi_{CG} = \tan^{-1}(z_{CG}/y_{CG}), \quad (8)$$

where r_{CG} denotes the magnitude of the CG offset from the barrel centerline and φ_{CG} the respective direction. Similarly, the magnitude of bullet tilt θ and its direction φ_θ are given by

$$\theta = \tan^{-1} \left(\frac{1}{e_{1,x}} \sqrt{e_{1,y}^2 + e_{1,z}^2} \right) \cong \sqrt{\alpha^2 + \beta^2}, \quad \varphi_\theta = \tan^{-1} \left(\frac{e_{1,z}}{e_{1,y}} \right) \cong \tan^{-1} \left(\frac{\beta}{\alpha} \right). \quad (9)$$

An illustration of the polar coordinate representation is given in Figure 5.

Magnitude and direction of the center of gravity (CG) offset and bullet tilt are presented in Figure 6 (blue lines). It is found that both the CG offset from the centerline and the in-bore tilt angle remain nearly constant after the bullet is fully engraved into the rifling profile, which is at about 1 ms. This indicates a regular transverse motion with the CG and the tilt rotating around the barrel centerline

according to the twist of the rifling. However, a small extent of high frequency oscillations is also observed, which is classically referred to as balloting. Hence, it is straightforward to split the bullet's transverse motion into two distinct components: a regular component caused by the twist of the rifling, and the "irregular" balloting part.

The regular motion is characterized by the following constraints: Magnitudes of CG offset and tilt angle remain constant

$$r_{CG,reg} = r_{CG,0}, \quad \theta_{reg} = \theta_0, \quad (10)$$

while the corresponding angular coordinates are dictated by the ratio of the projectile's axial position X to rifling twist rate L

$$\varphi_{CG,reg} = \frac{2\pi}{L}X + \varphi_{CG,0}, \quad \varphi_{\theta,reg} = \frac{2\pi}{L}X + \varphi_{\theta,0}. \quad (11)$$

The constants $r_{CG,0}, \theta_0, \varphi_{CG,0}, \varphi_{\theta,0}$ are obtained by a fitting procedure, which is applied from the time the bullet is fully engraved ($t \geq 1$ ms) until muzzle exit.

With the regular motion of the projectile's transverse motion fully defined, it is plotted in Figure 6 as a dashed orange line.

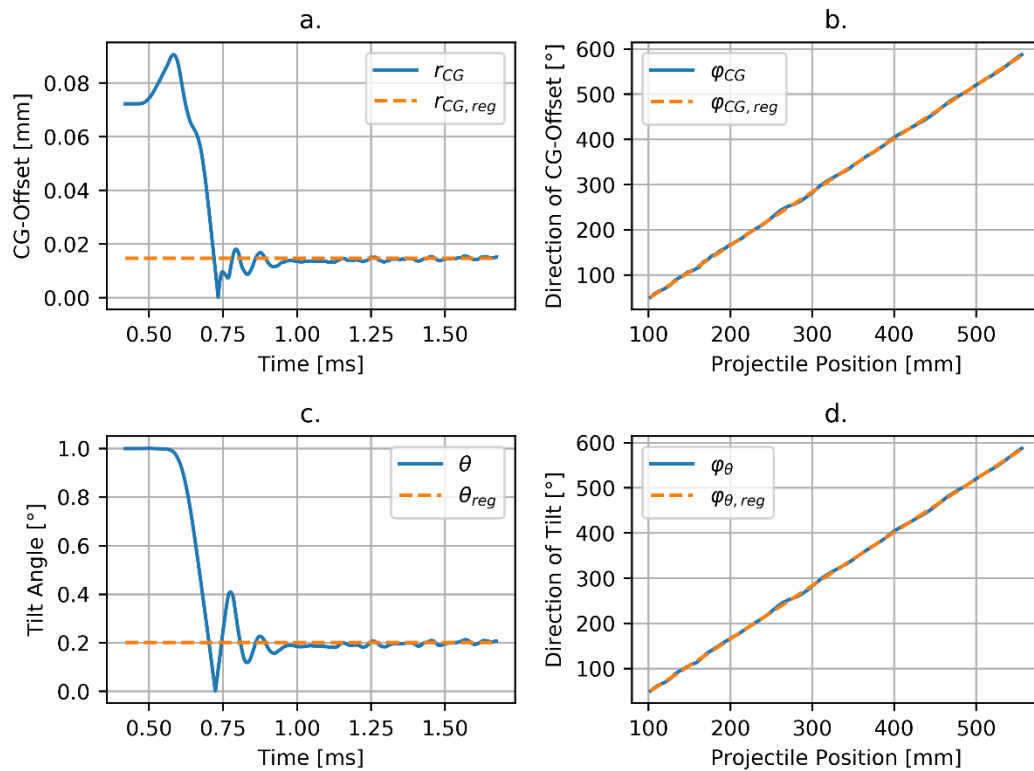


Figure 6. Magnitude and direction of CG offset and bullet tilt.

IRREGULAR TRANSVERSE MOTION

We postulate an additive decomposition of the projectile's transverse motion into a regular and an irregular (balloting) component

$$y_{CG} = y_{CG,reg} + y_{CG,irr}, \quad z_{CG} = z_{CG,reg} + z_{CG,irr}, \quad (12)$$

$$\alpha = \alpha_{reg} + \alpha_{irr}, \quad \beta = \beta_{reg} + \beta_{irr}. \quad (13)$$

As the regular motion is known from the previous section, the irregular component is found by a simple subtraction from the total motion (note that this has to be performed in Cartesian coordinates).

Regular and irregular components of the CG offset and bullet tilt are juxtaposed in Figure 7. The magnitudes of the irregular motion are obviously much smaller. Therefore, one may tend to assume that balloting is rather insignificant in this case. However, this is no longer true as soon as the respective rates are considered. As can be seen from Figure 8, the irregular transverse velocity and yaw rate are of a similar order of magnitude like their regular counterparts. Balloting can therefore not be neglected.

Muzzle Motion

The projectile's impact location is determined by its rigid body motion state at muzzle exit. Barrel vibrations contribute to the exit state in the way that the motion state of the muzzle is superimposed on the bullet's motion relative to the barrel. The muzzle motion is described by its transverse deflection, pointing direction, transverse velocity and angular rate. Transverse deflection and velocity are directly given by the FE model through position \vec{x}_N and velocity $\vec{v}_N = \dot{\vec{x}}_N$ of the foremost barrel segment N . The pointing direction is expressed by the unit vector

$$\vec{e}_M = \frac{(\vec{x}_N - \vec{x}_{N-1})}{\|\vec{x}_N - \vec{x}_{N-1}\|}. \quad (14)$$

For the muzzle's transverse angular velocity $\vec{\omega}_M$, rigid body kinematics yields

$$\vec{\omega}_M = \frac{(\vec{x}_N - \vec{x}_{N-1}) \times (\vec{v}_N - \vec{v}_{N-1})}{(\vec{x}_N - \vec{x}_{N-1}) \cdot (\vec{x}_N - \vec{x}_{N-1})} = \vec{e}_M \times \dot{\vec{e}}_M. \quad (15)$$

Assuming small angles again, the pointing vector is given by

$$e_{M,x} \cong 1, \quad e_{M,y} \cong \phi_M, \quad e_{M,z} \cong \psi_M, \quad (16)$$

where ϕ_M and ψ_M are the vertical and horizontal pointing angles. The angular velocity is then approximated by

$$\omega_{M,x} \cong 0, \quad \omega_{M,y} \cong -\dot{\psi}_M, \quad \omega_{M,z} \cong \dot{\phi}_M. \quad (17)$$

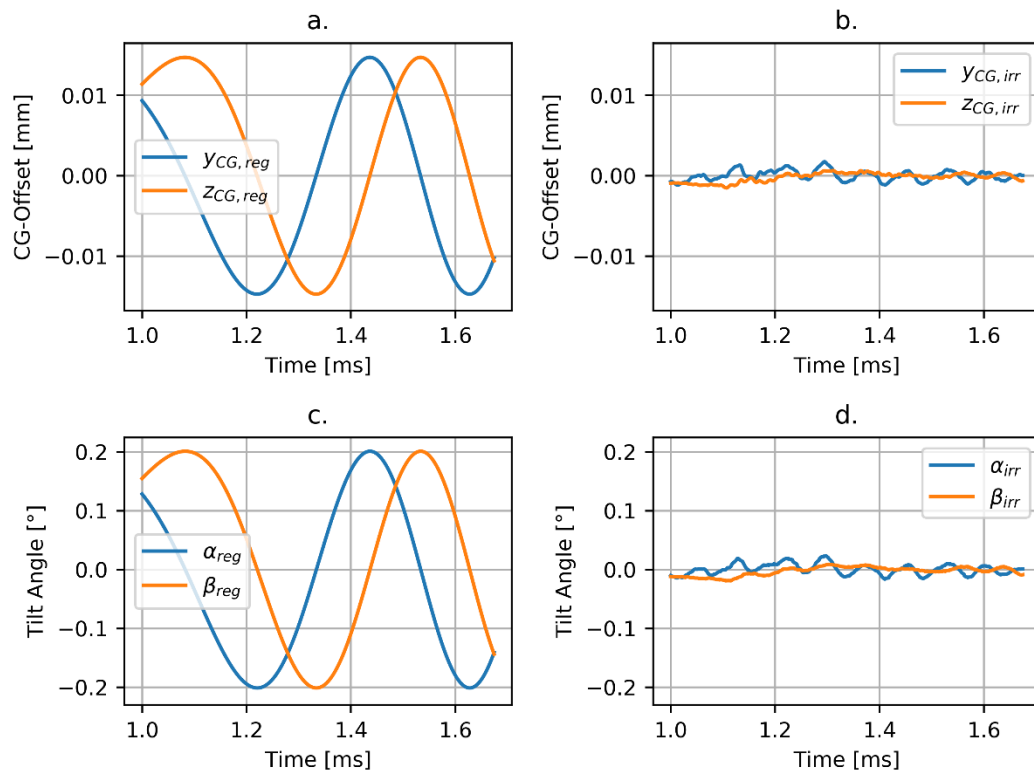


Figure 7. Regular and irregular components of CG offset (a., b.) and bullet tilt (c., d.).

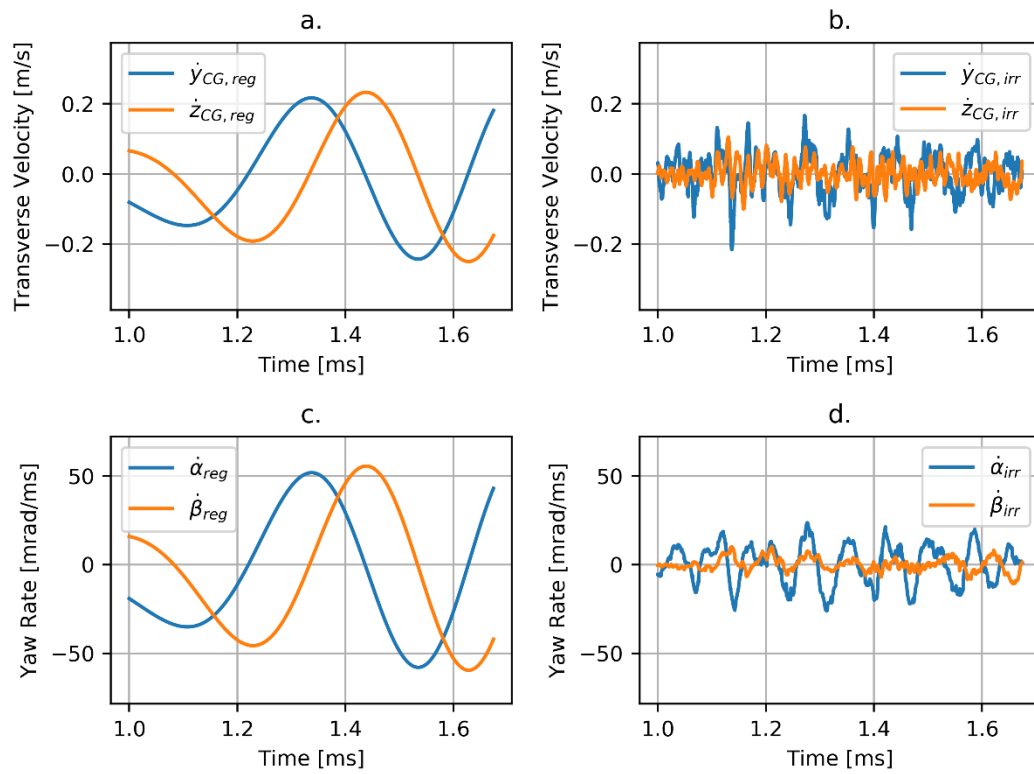


Figure 8. Regular and irregular components of transverse CG velocity (a., b.) and yaw rate (c., d.).

EVALUATION OF ACCURACY

Evaluation of target impact accuracy from FE in-bore simulations typically follows a straightforward approach: from the FE simulation of the launch cycle, one extracts the bullet's motion state at muzzle exit. This serves as the initial condition for a 6-DOF exterior ballistics calculation, which is used to determine the target impact location. The procedure is repeated for a number of simulations, where small asymmetries in geometry, mass distribution or loading of the projectile are realized in the FE model to take account of the stochastic perturbations occurring in reality. Finally, the resulting pattern of target impacts is condensed into a scalar measure of dispersion (e.g. standard deviation, average mean radius).

This approach of numerically predicting the dispersion of a specific weapon system is very common throughout literature [2, 5, 6, 7]. However, it has three drawbacks: firstly, the sole knowledge of the dispersion resulting from a sample of launch conditions provides very little insight into the mechanisms governing the formation of dispersion. In particular, it does not reveal whether the dispersion is caused by balloting, muzzle vibrations or by a regular off-axis motion of the projectile inside the barrel. Secondly, reliable statistics require large sample sizes, which makes the approach computationally expensive. Finally, the choice of launch conditions is usually very arbitrary, since data on the statistical distribution of perturbations is scarce.

The first of the drawbacks can be addressed by a separate evaluation of the dispersion for each of the three motion components.

To reduce the computational costs, one may wish to quantify the effect of a selected perturbation on accuracy from one single simulation, instead of performing a series of calculations with varying launch conditions. This simultaneously avoids the need for arbitrary assumptions on the statistical distribution of launch conditions.

The simplest way to quantify accuracy from a single simulation is to determine the deviation of the point of impact from the ideal, perturbation-free impact. This deviation can be expressed as

$$R_T = \sqrt{Y_T^2 + Z_T^2}, \quad (18)$$

where Y_T, Z_T are the impact coordinates relative to the ideal point of impact (the latter occurs if the projectile exits the barrel with zero transverse motion).

The impact location at a given target distance X_T depends on the projectile's transverse motion state at muzzle exit and can be calculated by means of 6-DOF exterior ballistics. An approximate solution is given by the "jump formula", which is derived in great detail in [8]

$$\begin{pmatrix} Y_T \\ Z_T \end{pmatrix} = X_T \left[\frac{1}{V_0} \begin{pmatrix} \dot{Y}_0 \\ \dot{Z}_0 \end{pmatrix} + \frac{C_{L\alpha}}{C_{M\alpha}} \frac{2\pi I_1}{L m d} \begin{pmatrix} -\beta_0 \\ \alpha_0 \end{pmatrix} - \frac{C_{L\alpha}}{C_{M\alpha}} \frac{I_2}{V_0 m d} \begin{pmatrix} \dot{\alpha}_0 \\ \dot{\beta}_0 \end{pmatrix} \right]. \quad (19)$$

The exit state is defined by the vertical and horizontal transverse velocities \dot{Y}_0 and \dot{Z}_0 , the pitch and yaw angles α_0 and β_0 and the respective rates $\dot{\alpha}_0$ and $\dot{\beta}_0$. The projectile velocity is denoted as V_0 . Variables related to projectile and barrel characteristics are

twist rate L , projectile mass m and diameter d , parallel and transverse moment of inertia I_1 and I_2 and the coefficients of lift force $C_{L\alpha}$ and overturning moment $C_{M\alpha}$.

However, in most cases, the deviation R_T is not a very indicative measure for target impact dispersion. The reason for this is that the bullet's exit state is commonly a very unsteady quantity, as balloting and muzzle motion are subject to heavy fluctuations. The slightest change in the system can therefore have a tremendous influence on the bullet's exit state. At this point, it is important to be aware that a ballistic system involves many factors, which are subject to chance. Especially variations in exit time are to be expected and must be considered in the evaluation of dispersion. This is done in the following, along with a separate treatment of regular, irregular and muzzle motion.

Regular Projectile Transverse Motion

Although quantifying dispersion by means of the deviation R_T is generally not recommended, it works well as long as only the regular motion is considered. In this case, the exit state is not affected by small changes in exit time, as the regular motion is free from any high frequency oscillations (see Figure 10a). What definitely has an influence on the impact location however, is the angular position of the (defective) cartridge inside the chamber. As the weapon itself is nearly symmetric (except for the finite number of lands), the direction of the impact deviation is solely determined by the angular position of the cartridge, while the magnitude R_T remains constant (see Figure 9). Note that, in a real gun, the cartridge's angular position is random. Hence, the target impact pattern for a given perturbation is represented by a circular ring with radius R_T . Impact deviation R_T , determined from a single simulation, is therefore a proper measure for the dispersion due to the regular projectile motion.

Irregular Projectile Transverse Motion

As the name suggests, the irregular component of the bullet's transverse motion is characterized by irregular high frequency oscillations (see Figures 7bd, 8bd). Therefore, the motion state at muzzle exit strongly depends on the exit time and the exact shape of the motion curve. Since neither of these is exactly reproducible from round to round, the exit state is random. The specific exit state obtained from a single simulation is therefore no longer a proper dispersion measure. As an elegant way to overcome this, we assume that each motion state in the vicinity of the muzzle exit is a potential exit state. Formula 19 is then applied to each motion state within a time interval close to muzzle exit, which yields a time dependent representation of the point of impact (see Figure 10b). Finally, statistical measures are applied on the resulting set of potential impact deviations $R_T(t)$, in order to determine a single number to quantify target impact dispersion. In this case, the 90 % quantile of $R_T(t)$ was used, which may be regarded as the radius of a circle containing 90 % of all potential impact points.

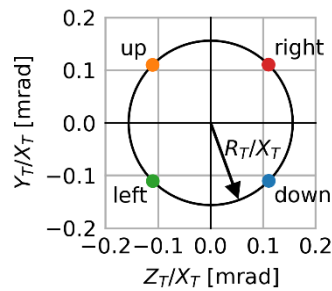


Figure 9. Target impact due to regular motion for different directions of initial bullet tilt.

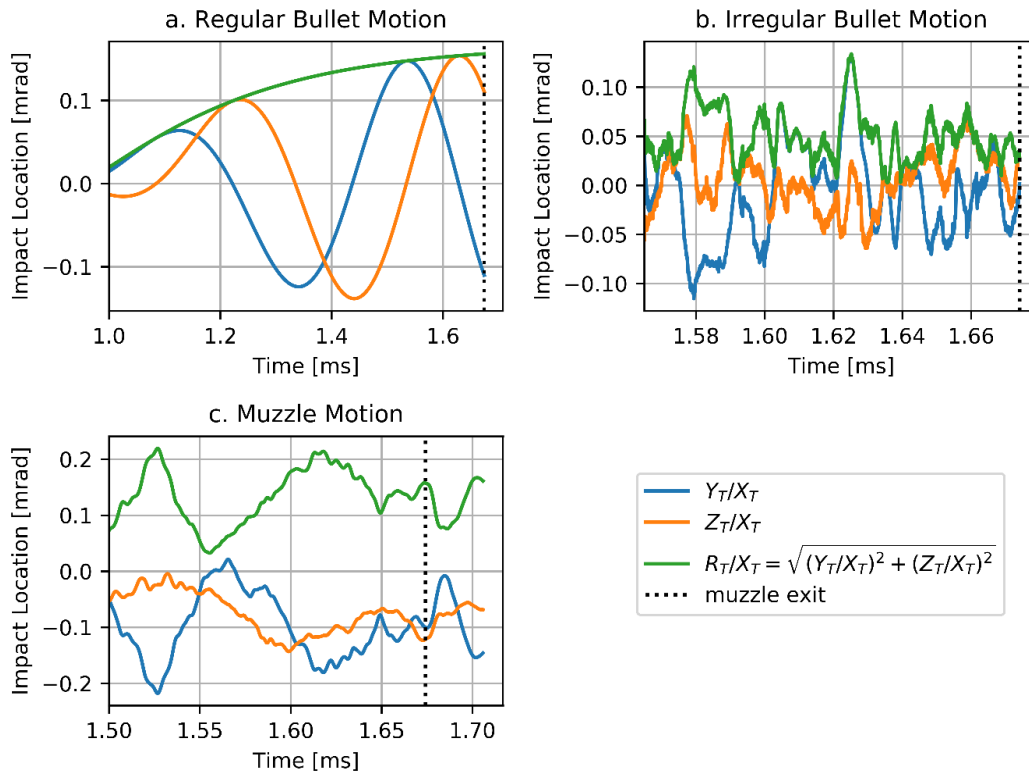


Figure 10. Relating the motion state of bullet and barrel during launch to target impact location.

Muzzle Motion

The evaluation of dispersion due to the muzzle vibrations follows the same procedure as for the irregular bullet motion. Again, each motion state within the vicinity of muzzle exit is converted into a time dependent point of impact (see Figure 10c). From the set of potential impact deviations $R_T(t)$, the 90 % quantile is calculated as a measure for the target impact dispersion due to muzzle vibrations.

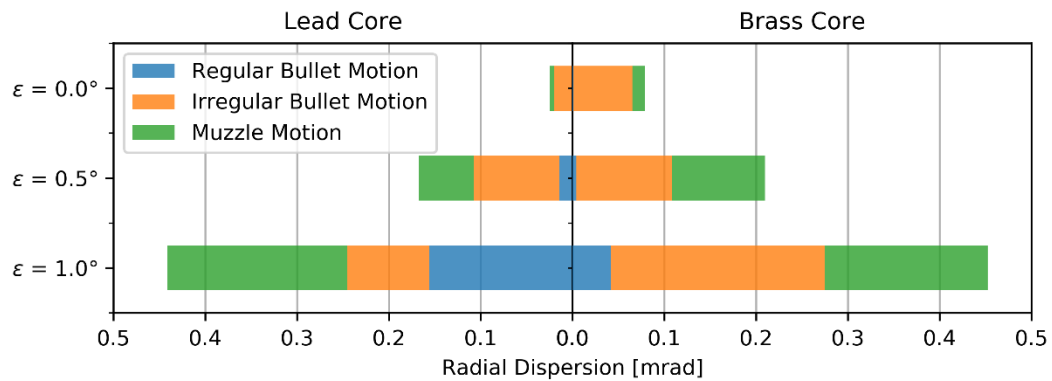


Figure 11. Effect of initial bullet tilt angle ϵ and bullet material on dispersion.

EXEMPLARY RESULTS

Figure 11 shows the effect of an initial bullet tilt on the respective dispersion due to the regular off-axis motion, irregular balloting and muzzle vibrations. The term “Radial Dispersion” refers to the dispersion measures derived in the previous section. As one would expect, dispersion values are generally higher for increasing angles of tilt. However, it is interesting to see, that the regular off-axis motion is massively reduced if the bullet core’s elastoplastic properties are changed from lead to brass (density was not altered in order to retain projectile mass). At the same time, the balloting-induced dispersion goes up, cancelling out the gain in overall accuracy. Similar findings have been reported by [5]. The dispersion due to muzzle vibrations is of a similar order of magnitude like the dispersion induced by projectile motion. It seems to be independent from the core material. Note that, in this case, the initial bullet tilt is the only cause of barrel vibrations, as no other deviations from ideal symmetry are present in the model.

CONCLUSION

A method for the postprocessing of Finite Element launch dynamics simulations in terms of target impact accuracy has been presented. The approach is based on a distinct separation of the bullet’s transverse motion during launch into a regular rotation caused by the rifling, irregular balloting oscillations and the muzzle motion. For each of these motion components, the influence on target impact accuracy is assessed. Note that estimations on accuracy are made from a single simulation, which is based on the assumption of stochastic variations in exit time. This is highly efficient, as it avoids the need for large series of simulations with varying launch conditions. So far, the approach has been used to study the effects of different types of perturbations on the accuracy of a generic 7.62 mm rifle. Future applications may also include large caliber weapons.

REFERENCES

1. Chevalier, O., M. Liennard, A. Langlet, Y. Guilnard, M. Mansion, and P. Bailly. 2017. "Dynamic of Tubes Crossed by High Speed Projectiles, Influence of Tube and Weapon Geometry on Accuracy and Dispersion," 30th ISB, Long Beach, US, 2017.
2. Newill, J., B. Guidos, and C. Livecchia. 2001. "Comparison between the M256 120-mm Tank Cannon Jump Test Experiments and ARL's Gun Dynamics Simulation Codes For Prototype KE," 10th Symposium on Gun Dynamics, Austin, US, 2001.
3. Eches, N., N. Paugain, and C. Doffemont. 2002. "In Bore Behavior of Large Calibre Armour Piercing Fin Stabilised Discarding Sabot Projectiles," 20th ISB, Orlando, US, 2002.
4. Eichhorst, C., D. Hopkins, M. Minnicino, and W. H. Drysdale. 2011. "Inclusion of Rifling and Variable Centerline in Gun Tubes for Enhanced Modeling of Launch Dynamics," 26th ISB, Miami US, 2011.
5. South J. and C. Eichhorst. 2016. "The Impact of Materials on the Launch Dynamics of Small Caliber Projectiles" 29th ISB, Edinburgh, UK, 2016.
6. Bulman, D. 1987. "A comparison of Theoretical Jump for Rifled and Non-Rifled Barrels," 5th Symposium on Gun Dynamics, Rensselaerville, US, 1987.
7. Newill, J., J. Garner, K. Soencksen, and C. Hoppel. 2001. "Launch Dynamics of the 120-mm M831A1 HEAT Training Projectile," 10th Symposium on Gun Dynamics, Austin, US, 2001.
8. McCoy, R. 1999. *Modern Exterior Ballistics: The Launch and Flight Dynamics of Symmetric Projectiles*. Atglen, US: Schiffer Pub., pp. 240-244.